applied sciences

MDPI

Article

The Potency of Graphitic Carbon Nitride (gC_3N_4) and Bismuth Sulphide Nanoparticles (Bi_2S_3) in the Management of Foliar Fungal Pathogens of Maize

Akinlolu Olalekan Akanmu [1], Timothy Oladiran Ajiboye [2,3], Masego Seleke [1], Sabelo D. Mhlanga [2], Damian C. Onwudiwe [3,4] and Olubukola Oluranti Babalola [1,*]

[1] Food Security and Safety Focus Area, Faculty of Natural and Agricultural Sciences, North-West University, Private Mail Bag X2046, Mmabatho 2735, South Africa
[2] Chemistry Department, Nelson Mandela University, University Way, Summerstrand, Gqeberha 6031, South Africa
[3] Material Science Innovation and Modelling (MaSIM) Research Focus Area, Faculty of Natural and Agricultural Sciences, North-West University, Mafikeng Campus, Private Bag X2046, Mmabatho 2735, South Africa
[4] Department of Chemistry, School of Physical and Chemical Sciences, Faculty of Natural and Agricultural Sciences, North-West University, Mafikeng Campus, Private Bag X2046, Mmabatho 2735, South Africa
* Correspondence: olubukola.babalola@nwu.ac.za

Abstract: Maize (*Zea mays* L.) is the most significant grain crop in South Africa. Despite its importance, the cereal is ravaged by several foliar fungal pathogens, which reduce maize quality and quantity at harvest. Hence, this study investigates the fungi associated with foliar diseases of maize in Molelwane, North-West Province, South Africa. The fungi were isolated, characterized and subjected to in vitro nanoparticle control. Samples of diseased maize leaves were aseptically collected from two maize-growing farms. Fungi associated with the samples were isolated and characterized using standard procedures. Bi_2S_3 (metal-containing) and gC_3N_4 (non-metallic carbon-based) nanoparticles were synthesized and used to challenge the pathogens using standard procedures. Foliar fungal pathogens isolated from the diseased maize leaves in this study were characterized as *Bipolaris zeicola, Phoma herbarum, Epicoccum nigrum, Alternaria alternata* and *Fusarium brachygibbosum. Phoma herbarium* > *A. alternata* > *B. zeicola* > *F. brachygibbosum* > *E. nigrum* was the order of percentage fungal inhibition by the nanoparticles. Bi_2S_3 was more effective against the pathogens at lower concentrations and gC_3N_4 at higher concentration levels. The two nanoparticle types evaluated in vitro shows potential for managing the foliar fungal pathogens, and this needs to be further validated in field studies.

Keywords: fungal characterization; DNA; nanoparticles; bismuth-based material; non-metallic material; plant disease management; South Africa

Citation: Akanmu, A.O.; Ajiboye, T.O.; Seleke, M.; Mhlanga, S.D.; Onwudiwe, D.C.; Babalola, O.O. The Potency of Graphitic Carbon Nitride (gC_3N_4) and Bismuth Sulphide Nanoparticles (Bi_2S_3) in the Management of Foliar Fungal Pathogens of Maize. *Appl. Sci.* **2023**, *13*, 3731. https://doi.org/10.3390/app13063731

Academic Editors: Andrea Ballini, Michele Covelli, Antonio Boccaccio, Maria Contaldo and Dario Di Stasio

Received: 8 February 2023
Revised: 8 March 2023
Accepted: 11 March 2023
Published: 15 March 2023

1. Introduction

Maize (*Zea mays* L.), which is the third most important crop across the world and the most significant grain crop in South Africa, is grown in diverse environments in the country [1,2]. Despite its importance, the crop is ravaged by a number of pathogenic microorganisms ranging from bacteria, fungi and viruses among others, which causes a diverse range of diseases that challenge plant health and reduce both the quantity and quality of the yield at harvest [3,4]. Among these disease-causing organisms, fungi occupy an important category owing to their short latent period, ease of spore dispersal and ability to sporulate prolifically and provide copious inoculum that could further infect plants [5]. Furthermore, their ability to infect a particular plant species is dependent on genes that differentiate the virulent fungi from their closely related nonvirulent relatives [6]. Fungi have been documented for their host specificity to maize and for causing diverse kinds of diseases such as ear and stalk rot caused by *Fusarium verticilliodes* [7], anthracnose stalk

rot *(Colletotrichum graminicola)*, *Aspergillus* ear and kernel rot (*Aspergillus flavus*), charcoal rot of maize (*Macrophomina phaseolina),* corn grey leaf spot disease (*Cercospora zeae-maydis),* southern corn leaf blight disease *(Bipolaris maydis)* and corn smut (*Ustilago maydis)* [8–13].

Foliar fungal pathogens of maize have been reported to cause major yield losses in maize fields across South Africa. Some of these include common rust, northern corn leaf blight, grey leaf spot and head smut diseases, among others [14,15]. Foliar diseases have been recorded as causing a high rate of severe damage in maize, with northern corn leaf blight disease alone capable of causing up to 50% production loss [16]. Furthermore, the development of secondary complications, which arise from severe foliar desiccation by the foliar pathogens, have been reported to result in severe lodging and up to 100% yield loss owing to stalk deterioration by grey leaf spot [16,17]. However, the management of foliar diseases can be complicated since multiple pathogens are involved in disease occurrences. Hence, foliar diseases of maize constitute a major threat to the sustainable production of this important cereal.

The management of the foliar diseases of maize with cultural methods such as tillage practices and crop rotations has only yielded limited effects [18–20]. Hence, reliance on fungicides, owing to their ease of application and efficacy, has been recorded previously over a range of pathogens [21–23]. However, their consequent harmful impact on the soil and human health necessitates the need to explore other promising alternatives, such as nanoparticles [24]. Nanoparticles are small particles that range between 1 to 100 nanometres in size, which are specially prepared from the active ingredients of the source materials to enhance their efficiency [25,26]. They have been employed as nano-phytopathology for detecting, diagnosing and controlling plant diseases and their pathogens [27–29]. The action of the nanoparticles against fungal pathogens is by the inhibition of biofilm formation, destruction of cell walls, destruction of cell membranes or interaction with biomolecules [28,30]. Hence, the application of nanoparticles was considered essential in this study since foliar diseases of maize at Molelwane, North-West Province of South Africa, have persisted over a range of management practices, from cultural to the use of chemical control. This study therefore set out to characterize the fungal pathogens associated with the foliar diseases of maize and evaluate their in vitro control using bismuth sulphide nanoparticles (Bi_2S_3) and graphitic carbon nitride nanoparticles (gC_3N_4). Bismuth sulphide is a metal-containing chalcogenide nanoparticle, while graphitic carbon nitride is a non-metallic, carbon-based nanoparticle. As far as we know, this is the first report on the use of these two nanoparticle types for combating foliar fungal pathogens of maize.

2. Materials and Methods

2.1. Sample Collection and Fungal Isolation

Maize leaf samples were aseptically collected from the North-West University Agricultural Research Farm in Molelwane on March 2022 (25°47′26.4″ S 25°37′01.6″ E). From the two maize fields sampled at the research farm, leaf samples were collected from maize plants showing leaf blight diseases at three replicates per sample. The samples were separately packed in zip-lock bags and carried in an ice box to the laboratory where the leaves were rinsed in running tap water, cut into manageable pieces, sterilized in 5% NaOCl, and rinsed in three exchanges of sterile distilled water. The leaves were allowed to dry under a lamina flow hood and then plated in potato dextrose agar (PDA) poured plates. At 28 °C, the plates were incubated for a period of seven days under 12 h/12 h cycles of light and dark and observed for fungal growth. Isolates with similar morphological characteristics such as the growth rate, growth patterns, colour and morphological appearance were grouped together. The isolates were sub-cultured to obtain a pure culture of each fungal isolate, and the stock inoculums were prepared and stored at −4 °C. Other chemical reagents used for the synthesis of the nanoparticles were para-tolualdehyde (CAS-4702-76-5), 4-ethylaniliine (CAS-589-16-2), ethanol (CAS-64-17-5), methanol (CAS-67-56-1), dichloromethane (CAS-75-09-2), sodium hydroxide (CAS-1310-73-2), carbon disulphide (CAS-75-15-0), ammonium hydroxide (1336-21-6), bismuth (III) nitrate pentahydrate (CAS-10035-06-0), melamine

(108-78-1) and dimethyl sulfoxide (DMSO) (CAS-67-68-5). They were used in pure form as sourced from Sigma Aldrich.

2.2. Molecular Characterization of the Isolated Fungi

2.2.1. Extraction and Amplification of Genomic DNA

Each fungal isolate was grown on PDA at 28 ± 2 °C for 5 days. The extraction of fungal DNA was then conducted using the Quick-DNA Fungal/Bacterial Miniprep Kit, in line with the manufacturer's manual instructions (Zymo Research, Irvine, CA, USA). The extracted fungal genomic DNA was subjected to PCR amplification of the internal transcribed spacer (ITS) region of the ITS1-5.8S-ITS2 rDNA gene, as described by Daccò, et al. [31]. The primers used were ITS1 (5′-TCCGTAGG TGAACCTGCGG-3′) and ITS4 (5′ TCCTCCGCTTATTGATATGC-3′). The PCR reaction was performed on a Thermocycler Bio-Rad T100 in a 25 µL reaction mixture containing 1× DREAM Taq Green PCR MasterMix reaction buffer (Thermo Scientific, Pittsburg, PA, USA) (12.5 µL), 1 µL (10 µM) of each primer, 2 µL of the DNA sample, and 9.5 µL of nuclease-free water. The PCR program was as follows: denaturation by heating for 5 min at 95 °C; 35 cycles of 30 s at 95 °C, 45 s at 50 °C, and 1 min at 72 °C; and a final elongation step for 10 min at 72 °C. The PCR products obtained were purified with ExoSAP-IT (Applied Biosystems, Foster City, CA, USA) according to the manufacturer's protocol. After the PCR process, gel electrophoresis was conducted to allow imaging of the separated DNA molecules, using the Chemidoc^{TM} imaging system (BIO-RAD Laboratories, Hercules, CA, USA). The amplified and purified DNA was sequenced at Inqaba Biotechnology Pty, Pretoria, South Africa. The sequences were compared with target sequences on the NCBI database, and MEGA X 10.1.7 was used for phylogenetic tree construction.

2.2.2. Phylogenetic Analysis

BioEdit software version 7.0.5 was used for pairwise contrast and multiple alignments to determine similarities and differences among the nucleotides. Pairwise affinity values were calculated, and phylogenetic trees were constructed using the neighbour-joining method with the Tamura–Nei parameter as a substitution model, as implemented in MEGA X 10.1.7. The reliability of internal branches was assessed using the bootstrap method with 1000 replicates. The consensus nucleotide sequence data from this investigation were deposited in GenBank with the following accession numbers OP536174–OP536199 (Table 1).

Table 1. 16 s rRNA gene sequence-based identification of the isolates and their accession numbers.

Accession Code	Isolate Name	Accession Number	Blastn, Closest Relative	Relative Accession	Similarity %	E Value
AD1	*Bipolaris zeicola strain 1*	OP536177	*Bipolaris zeicola*	MK841439	99.81	0.0
AD6	*Phoma herbarum strain 1*	OP536178	*Phoma herbarum*	MT420621	100	0.0
AH1	*Epicoccum nigrumisolate*	OP536185	*Epicoccum nigrum*	MT582797	100	0.0
BD5A	*Alternaria alternata strain 2*	OP536192	*Alternaria alternata*	MN249500	100	0.0
BD2	*Fusarium brachygibbosum*	OP536195	*Fusarium brachygibbosum*	KY024400	100	0.0

After the genomic sequencing, the fungi were identified up to the subgroup level utilizing the ITS areas of the ribosomal DNA, and an analysis of the phylogenetic relationship of the generated sequences was conducted to identify the various identities of the isolated fungi. This was executed through the nucleotide BLAST algorithm and program of the NCBI. The highest percentage of matches obtained implied that the matches were most likely isolated fungi.

3. Synthesis and Characterization of the Nanoparticles

3.1. Synthesis and Characterization of Bismuth Sulphide

The bismuth sulphide was prepared from the thermal decomposition of the bismuth (III) dithiocarbamate complex. The first stage involved the preparation of the dithio-

carbamate complex of bismuth. This stage started with the reaction of equal moles of p-tolualdehyde and 4-ethylaniline dissolved in a flask by using ethanol as a solvent. The content of the flask was stirred for 3 h under ice, and the solvent was evaporated to obtain an oil-like product. The oily product obtained was dissolved in a solution containing 1:1 methanol and dichloromethane. Then, 13.8 mmol of sodium borohydride was introduced into the flask. This was first stirred for 2 h under ice, immediately followed by 24 h stirring at room temperature.

After this, the solvent was evaporated by raising the temperature to 40 °C. The product obtained at this stage was washed with distilled water and extracted with dichloromethane via the use of a separating funnel. The organic phase was evaporated by stirring at 40 °C again to obtain a light-yellow oil. The oil obtained (4 mmol) was dissolved in ethanol in a clean flask and 4 mmol of carbon disulphide was added. The pH of the content of the flask was altered by adding 10 mL of NH_4OH. The whole content was stirred for 2 h 15 min then 1.67 mmol of hydrated bismuth nitrate was introduced and stirred for 12 h. The resultant creamy solution was filtered under pressure and left to dry to obtain the bismuth (III) dithiocarbamate.

The second stage involved the thermal decomposition of the dithiocarbamate. A solvothermal reaction was employed under an atmosphere of nitrogen. Briefly, 1.00 g of the dithiocarbamate complex was introduced into a 3-necked round bottom flask and 20 mL of oleylamine was added. The mixture was steadily heated until it reached 180 °C and it was maintained at this temperature for 1 h. After the reaction was complete, the flask was allowed to cool to room temperature, and then the product obtained was washed by centrifugation with ethanol and toluene. The pure product was dried in an oven set at 80 °C for 6 h. This final product was kept for characterization. The entire synthetic processes have been summarized in Figure 1.

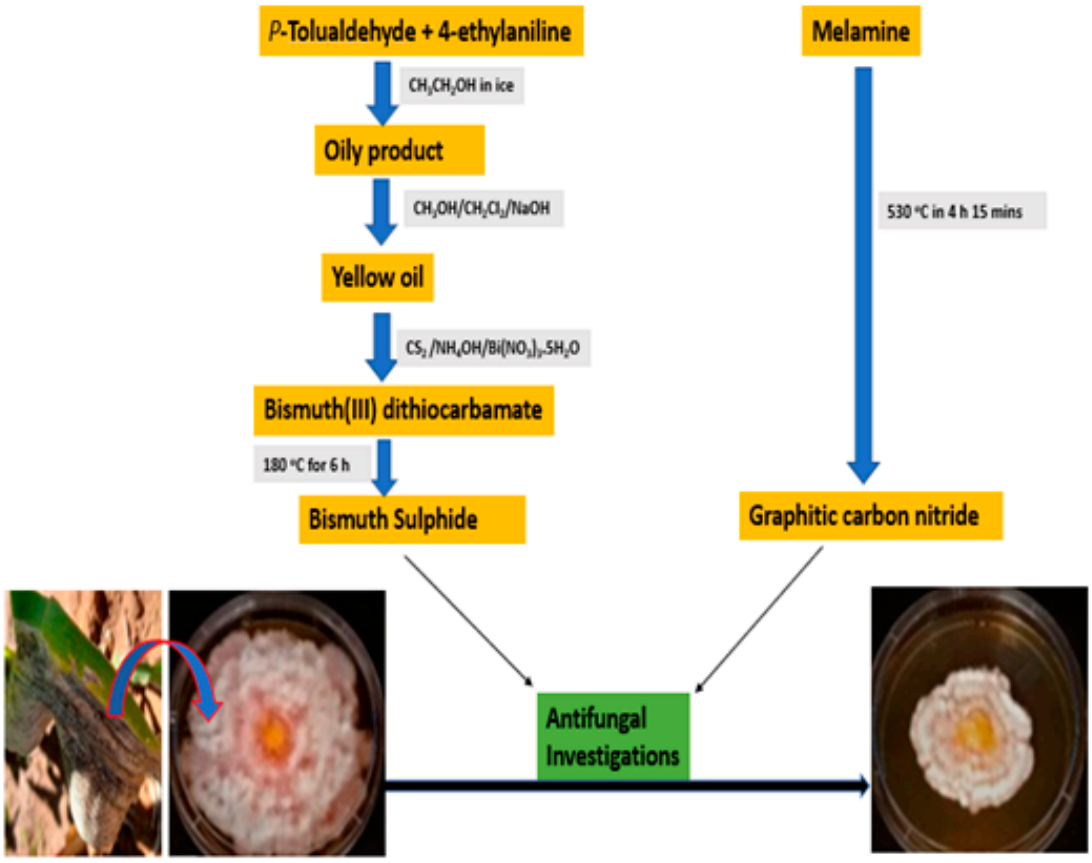

Figure 1. Synthesis of bismuth sulphide and graphitic carbon nitride used for the antifungal treatment of foliar fungi of maize.

One of the most powerful and non-destructive tools for the structural characterization of materials is X-ray diffraction (XRD) [32]. The structural identification of bismuth sulphide was carried out in the range of 0° to 80° 2θ angle. As shown in Figure 2, all the peaks are the characteristic peaks of the orthorhombic lattice structure of bismuth sulphide, having a space group of *Pbnm (62)* (JCPDS card 17-0320) [33]. Prominent among these peaks are (130), (211) and (221) at 24.9°, 28.6° and 31.8°, respectively. The pattern obtained perfectly matched that of an earlier report [34]. No peak from either bismuth or sulphur was observed on the XRD spectrum and the high intensity of the peaks showed that the as-synthesized Bi_2S_3 had high crystallinity [35].

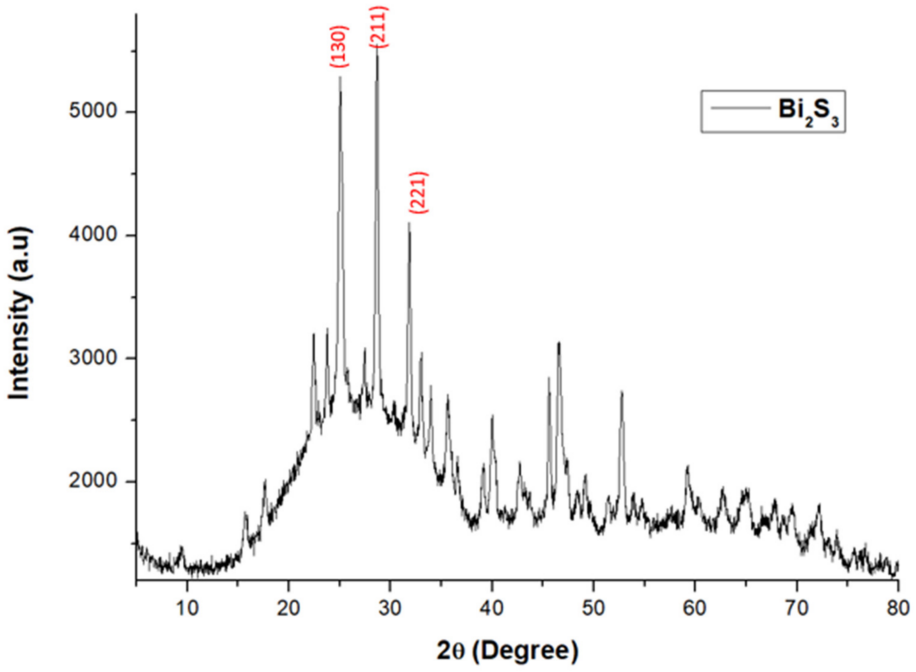

Figure 2. The XRD spectrum of bismuth sulphide. The prominent peaks are indexed in red color.

To further confirm the formation of bismuth sulphide, an EDS analysis was carried out. As shown in Figure 3a, the two elements in the nanoparticles are bismuth and sulphur with a mean relative abundance of 81.96% and 18.04%, respectively. Based on the percentage abundance, the ratio of the mole of bismuth to sulphur is 3:1. This shows the formation of bismuth sulphide. The fact that there is no other element on the spectrum further confirms the purity of the synthesized bismuth sulphide. Further probing into the internal morphology of the synthesized bismuth sulphide nanoparticles showed that it has a rod-like structure (Figure 3b).

3.2. Synthesis of Graphitic Carbon Nitride

Graphitic carbon nitride was obtained by the thermal decomposition of melamine [36,37]. Briefly, 10.00 g of melamine was accurately measured into a crucible. The crucible was closed to prevent the oxidation of heteroatoms in melamine to gaseous pollutants. The crucible with its content was placed inside a muffle furnace and maintained at 530 °C for 4 h 15 min. At the completion of the reaction, the crucible was allowed to cool down to room temperature and a yellow lump was obtained. The lump was crushed with a pestle and mortar to obtain a powder with a high surface area. The powder was protected from moisture by keeping it in the desiccator. We have discussed and previously published the detailed characterization of graphitic carbon nitride [38,39]. The reader is referred to these previous publications for detailed characterization of the graphitic carbon nitride used for the present investigations.

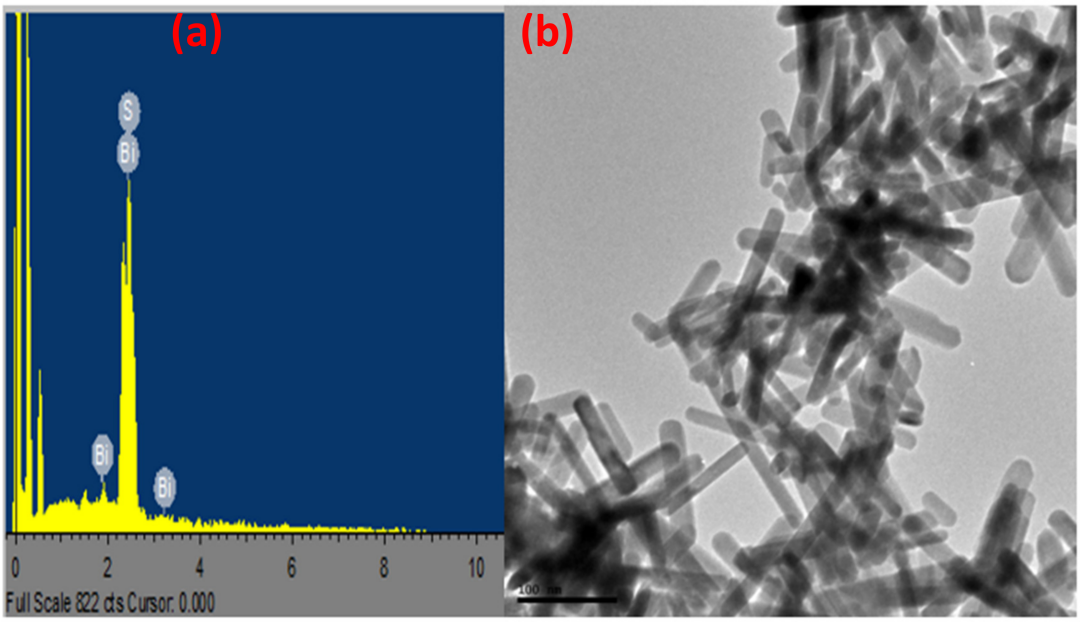

Figure 3. (**a**) EDS spectrum of bismuth sulphide showing the presence of bismuth and sulphur only in the as-prepared nanoparticles and (**b**) TEM spectrum of bismuth sulphide showing a nanorod internal morphology.

4. Nanoparticle Management of Fungi

The nanoparticles of bismuth sulphide (Bi_2S_3) and graphitic carbon nitride (gC_3N_4) were dissolved in 20% dimethylsulfoxide (DMSO) then diluted in 80% sterile distilled water according to the method described by Akanmu, et al. [40], and further prepared into 5, 10 and 15 mg/mL concentration levels. Assessment of the antifungal activity of the nanoparticles was carried out on PDA media supplemented with 20 µL of nanoparticles in each 15 mL PDA media plate at each concentration level. On each plate the respective fungal growths of AD1, AD6, AH1, BD5A and BD2 were inoculated at the centre of the plates using a 5 mm cork-borer. The cultured plates were incubated at 28 ± 2 °C. In the control plates, the media were only supplemented with corresponding levels of DMSO, without any nanoparticles. The growth of the fungi was monitored for 2 weeks, and the fungal diameter was measured at 3 days intervals. The percentage inhibition rate was calculated according to the method described by Olowe, et al. [41] as:

$$\%growth = \frac{D_c - D_t}{D_c} * 100$$

where:

D_t = Diameter of the fungi inoculated in a nanoparticle-supplemented PDA plate
D_c = Diameter of the fungi without a nanoparticle-supplemented PDA plate (control)

Statistical Analysis

Data collected on each replicate were subjected to analyses of variance (ANOVA), using Statistical Analysis Software (SAS 2003), while means were separated using Duncan's Multiple Range Test. All analyses were performed at a 5% ($p \leq 0.05$) level of significance.

5. Results

Five pathogenic fungi associated with corn leaf blight disease were isolated. The fungi were identified morphologically (Figure 4) and molecularly by using PCR-ITS amplification of the rRNA gene. The blast search on the NCBI was identified as AD1 *Bipolaris zeicola strain 1*, AD6 *Phoma herbarum strain 1*, AH1 *Epicoccum nigrum*, BD5 *Alternaria alternata strain 2* and BD2 *Fusarium brachygibbosum* (Table 1).

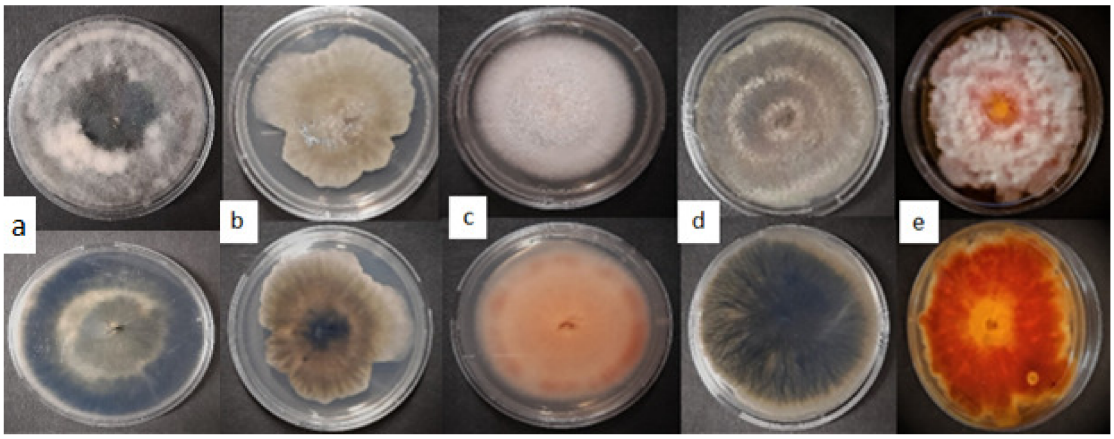

Figure 4. Front and back view of the fungal isolates (**a**) Bioplaris zeicola, (**b**) Phoma herbarum, (**c**) Epicoccum nigrum, (**d**) Alternaria alternata, (**e**) Fusarium brachygibbosum.

Sequences of the isolated fungal strains were aligned with those earlier documented on the NCBI platform. The phylogenetic relationship tree of the isolates revealed AD6 clustered into a distinct, well-supported clade with *Phoma herbarum* MT420621, AH1 clustered with *Epicoccum nigrum* MT582797, BD2 with *Fusarium brachygibbosum* KY024400, and BD5A with *Alternaria alternata* MN249500, while AD1 clustered with a clade supported by *Bipolaris zeicola* MT841439 (Figure 5).

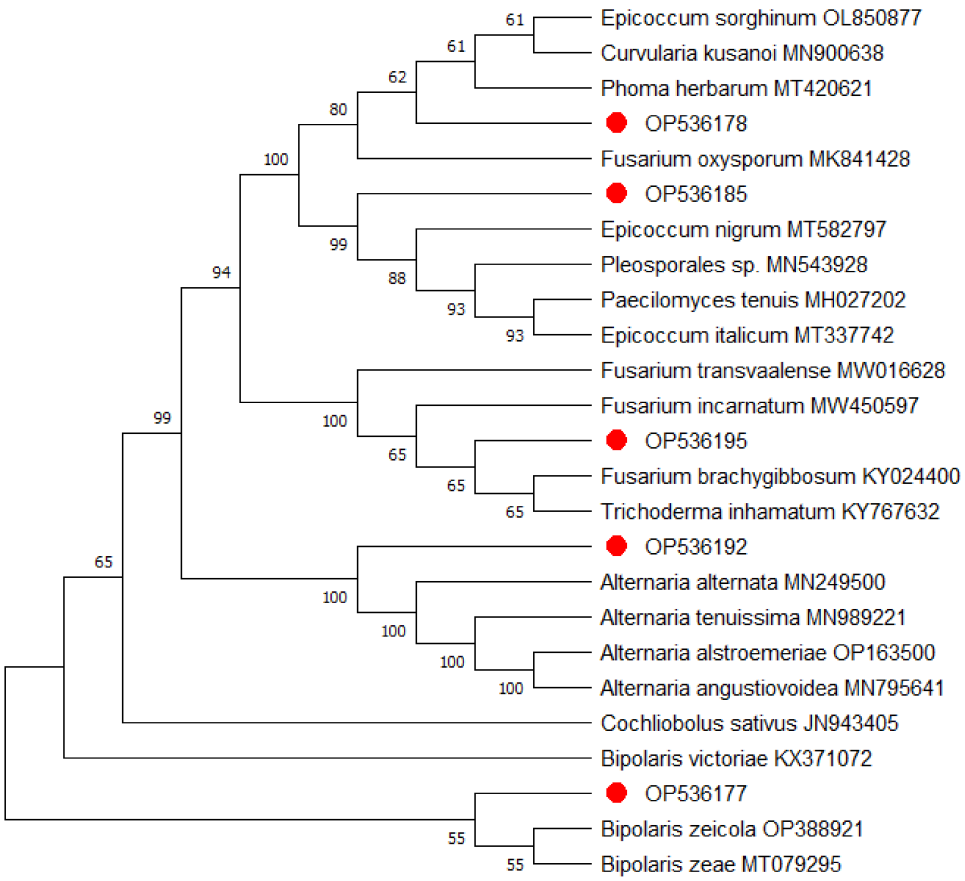

Figure 5. The phylogenetic relationships between the isolated pathogenic fungi and selected database relatives on the NCBI generated through transcribed spacer (ITS) rRNA genes, analysed via Kimura's two-parameter models. Bootstrap support values higher than 50% from 1000 replicates are shown at the nodes. *Bipolaris zeae* (MT079295) was used as the out-group.

The percentage inhibition of the Bismuth sulphide nanoparticles against the evaluated fungi showed *Phoma herbarun* (35.72%), *Bipolaris zeicola* (31.58%) and *Alternaria alternata* (28.86%) were the most significant ($p < 0.05$) at 5 mg/mL concentration. *Alternaria alternata* (37.56%) produced the most significant result at 10 mg/mL, while 2 fungi, *Phoma herbarum* (39.71%) and *A. alternata* (35.35%), recorded the most inhibition at 15 mg/mL. Similarly, results obtained from the graphitic carbon nitride nanoparticles showed its effectiveness against *Phoma herbarum* at 5 mg/mL (45%) and at 10 mg/mL (65.64%), while *P. herbarum* (41.03%) and *A. alternata* (34.33%) showed the most significant inhibition at 15 mg/mL, a performance that was followed by *Fusarium brachgibbosum* and *Bipolaris zeicola* at a similar level of significance ($p > 0.05$) (Table 2).

Table 2. Percentage inhibition of different concentrations of nanoparticles on the growth of some pathogenic fungi.

Organisms	Bi_2S_3			gC_3N_4		
	5 mg/mL	**10 mg/mL**	**15 mg/mL**	**5 mg/mL**	**10 mg/mL**	**15 mg/mL**
Bioplaris zeicola	31.58 ± 3.30 a	28.49 ± 2.53 b	16.97 ± 2.63 b	13.23 ± 2.80 c	15.44 ± 2.81 b	18.53 ± 4.12 b
Phoma herbarum	35.72 ± 4.03 a	21.09 ± 2.95 c	39.71 ± 2.90 a	45.00 ± 3.97 a	65.64 ± 2.32 a	41.03 ± 3.21 a
Epicoccum nigrum	4.59 ± 1.21 c	7.58 ± 1.61 e	7.54 ± 1.71 c	5.27 ± 1.37 d	5.09 ± 1.50 c	9.06 ± 1.34 c
Alternaria alternata	28.86 ± 5.35 a	37.56 ± 1.82 a	35.35 ± 1.87 a	28.63 ± 2.12 b	20.42 ± 3.17 b	34.33 ± 1.79 a
Fusarium brachygibbosum	14.00 ± 2.54 b	14.13 ± 2.78 d	16.54 ± 2.92 b	7.92 ± 2.90 dc	20.58 ± 2.54 b	19.37 ± 2.43 b
LSD	7.96	6.31	5.43	6.13	6.85	7.47

Means with different letters across the column are significantly ($p < 0.05$) different. Bi_2S_3 = Bismuth sulphide nanoparticles, gC_3N_4 = Graphitic carbon nitride nanoparticles.

The pooled effect of the two nanoparticle types against the tested fungi showed *Phoma herbarum* (40.36%, 43.37% and 40.37%), followed by *Alternaria alternata* (28.74%, 28.99%, and 34.84%) and *Bipolaris zeicola* (22.40%, 21.96% and 17.75%) as the most significantly inhibited fungi across the concentration levels, respectively (Table 3).

Table 3. Percentage inhibition of the pooled effect of nanoparticles on the fungi growth.

Organisms	5 mg/mL	10 mg/mL	15 mg/mL
Bioplaris zeicola	22.40 ± 2.53 c	21.96 ± 2.10 c	17.75 ± 2.42 c
Phoma herbarum	40.36 ± 2.88 a	43.37 ± 3.74 a	40.37 ± 2.14 a
Epicoccum nigrum	4.93 ± 0.90 e	6.33 ± 1.10 d	8.30 ± 1.08 d
Alternaria alternata	28.74 ± 2.85 b	28.99 ± 2.20 b	34.84 ± 1.28 b
Fusarium brachygibbosum	10.96 ± 1.96 d	17.35 ± 1.92 c	17.96 ± 1.89 c
LSD	5.27	6.44	4.61

Means with different letters across the column are significantly ($p < 0.05$) different.

Phoma herbarium > *A. alternata* > *B. zeicola* > *F. brachygibbosum* > *E. nigrum* was the order of fungal inhibition by the pooled effect of the nanoparticles at all the concentration levels observed (Figure 6). Bi_2S_3 nanoparticles showed a higher percentage inhibition (22.95%) than gC_3N_4 nanoparticles at 5 mg/mL. However, gC_3N_4 nanoparticles recorded better performances (25.43% and 24.46%) at 10 mg/mL and 15 mg/mL concentrations, respectively (Figure 7).

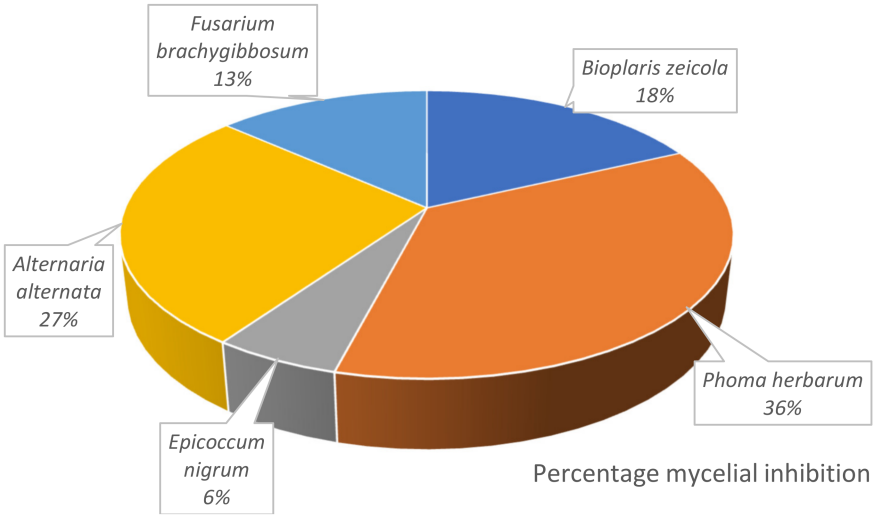

Figure 6. Pie chart showing the pooled effect of the nanoparticles on the percentage mycelial inhibition.

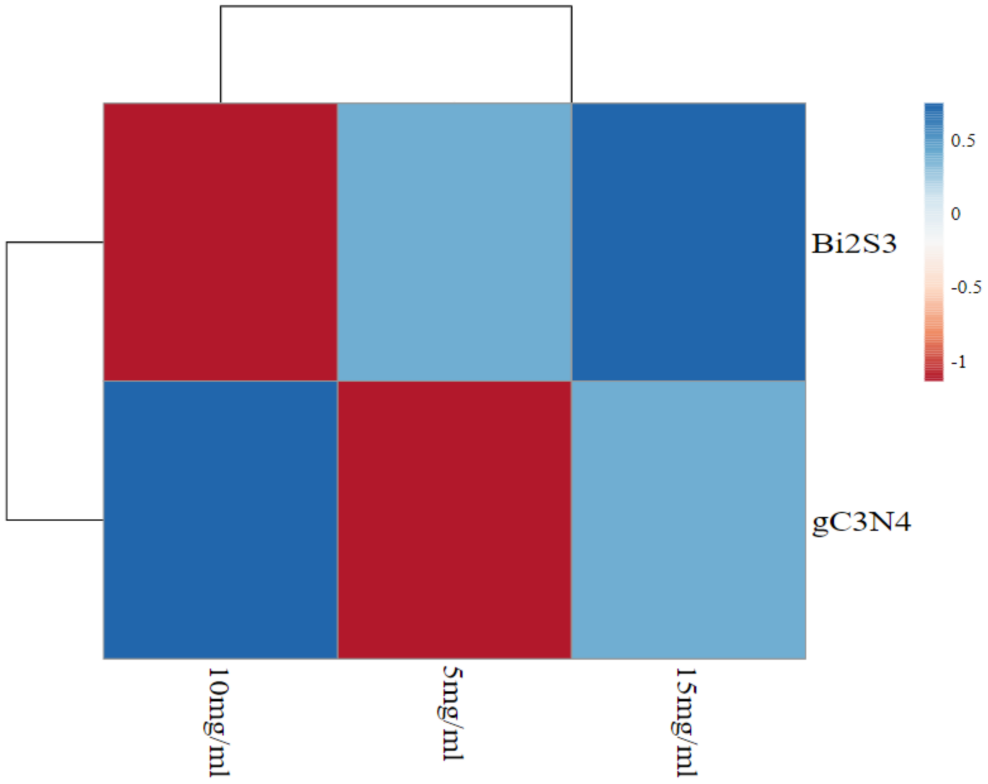

Figure 7. Heatmap showing performances of the two nanoparticle types at different concentration levels.

The most significant nanoparticle inhibition of fungal growths was obtained at day 3 after culturing. No significant ($p > 0.05$) difference was recorded in the fungal growths inhibited by Bi_2S_3 nanoparticles at 5 mg/mL and 10 mg/mL concentrations on days 3, 5, 7 and 9, while the least inhibition at 15 mg/mL was recorded on day 9 of observation. Also, with the gC_3N_4 nanoparticles, the percentage inhibition on day 5 significantly followed performances recorded on day 3 across all the concentration levels, while days 7 and 9 showed no significant differences in the fungal growth inhibition (Table 4).

Table 4. Effects of experimental duration (days) on the nanoparticle inhibition of fungi.

Days	Bi_2S_3			gC_3N_4		
	5 mg/mL	**10 mg/mL**	**15 mg/mL**	**5 mg/mL**	**10 mg/mL**	**15 mg/mL**
3	30.41 ± 4.21 a	29.32 ± 2.52 a	31.97 ± 2.98 a	26.97 ± 3.81 a	31.71 ± 4.90 a	30.27 ±3.21 a
5	22.80 ± 3.24 b	21.34 ± 2.35 b	25.10 ± 2.66 b	21.82 ± 3.59 ba	26.27 ± 4.63 ba	25.82 ± 2.86 ba
7	19.65 ± 3.91 b	19.07 ± 3.13 b	20.28 ± 3.17 cb	16.40 ± 3.62 bc	21.41 ± 3.91 b	22.88 ± 3.23 b
9	18.94 ± 3.61 b	17.35 ± 2.99 b	15.53 ± 2.96 c	14.85 ± 3.35 c	22.35 ± 4.17 b	18.88 ± 3.38 b
LSD	7.12	5.65	4.85	5.48	6.13	6.68

Means with different letters across the column are significantly ($p < 0.05$) different. Bi_2S_3 = Bismuth sulphide nanoparticles, gC_3N_4 = Graphitic carbon nitride nanoparticles.

The pooled effect of nanoparticles on the fungal inhibition showed no significant ($p < 0.05$) difference in the results obtained at all concentration levels on days 3, 5 and 7, while the results produced at a concentration of 10 mg/mL were more significant on day 9 (Figure 8).

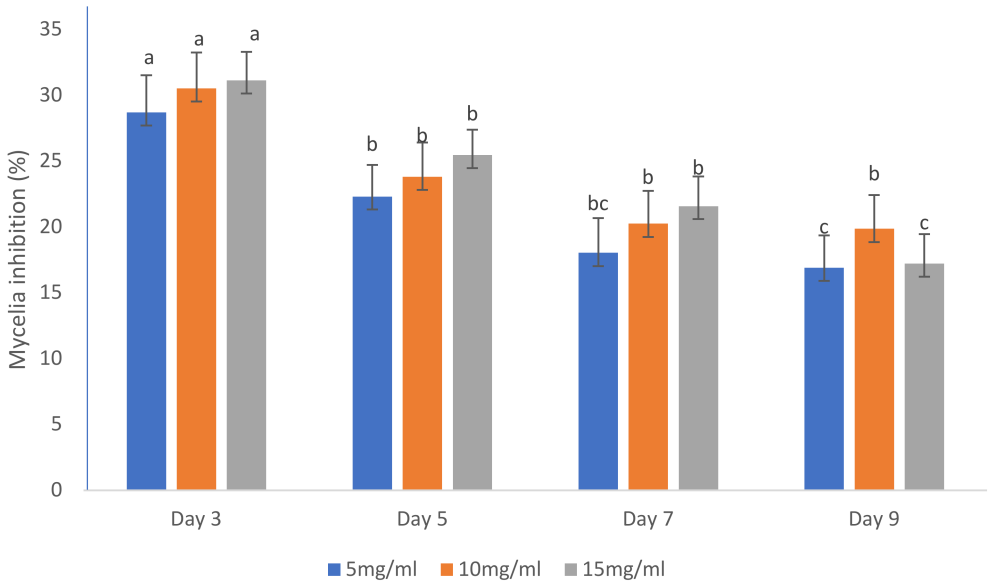

Figure 8. Heatmap showing the effect of days of observation on the percentage of fungal inhibition at different concentration levels. Means with different letters across the days are significantly ($p < 0.05$) different.

6. Discussion

The fungal pathogens isolated from the corn leaf blight disease of maize in Molelwane, North-West Province of South Africa, were characterized as *Bipolaris zeicola, Phoma herbarum, Epicoccum nigrum, Alternaria alternata* and *Fusarium brachygibbosum. Bipolaris zeicola,* earlier identified as *Cochliobolus carbonum,* is from the phylum Ascomycota and family Pleosporales. Selections from these populations have been predicted to keep evolving, especially in seed fields where novel pathotypes with distinctive lesions, toxins, and/or genotype specificity are present [42]. Some of its races have been previously implicated with the Helminthosporium leaf spot disease of maize [43], maize root rot [44], northern corn leaf spot, and northern and Southern corn leaf blight disease [45], while it has been found as the causal agent of leaf blight disease on the invasive grass *Microstegium vimineum* [46].

Phoma has been reported as the largest and the most widely distributed genus of the order Pleosporales [47]. Its species have reportedly thrived in various habitats where they have occurred as saprophytes, epiphytes, parasites and hyperparasites [48]. *Phoma herbarum,* which was recently reclassified as *Phoma sensu stricto,* has been reported to attack crop plants, producing symptoms such as root rot, leaf blight and the wilting of

the host plant [47]. The fungus has also been found to cause leaf spot disease of purple coneflower (*Echinacea purpurea*) in Northern Italy [49].

Similarly, fungi, including *Epicoccum, Fusarium* and *Alternaria* species, also have multiple habitats, and they colonize the stems, leaves and areas of the plants. Thus, plant leaves in tropical forests have been found to contain numerous independent infections, which are of high diversity [50]. *Alternaria alternata* has been found as the cause of leaf blight of maize in China [51], and also in sunflower cultivation in South Africa, especially where sunflower is grown in rotation with maize [52]. Although *Fusarium brachygibbosum* has been considered a plausible candidate for deployment as a bioagent for *Striga hermonthica* management in sorghum [53], other races of *Fusarium brachygibbosum* have been implicated in maize stalk rot [54]. Similarly, the report of Taguiam, et al. [55] revealed a total of 18 species of *Epicoccum,* which are pathogens to 46 different plant species in about 20 countries where they mostly cause leaf spot disease. However, there are five other *Epicoccum* species (*E. nigrum, E. layuense, E. dendrobii, E. mezzettii*, and *E. minitans*) with biological control capabilities against different plant pathogens, with *Epicoccum nigrum*, as the most promising of the five. This claim was verified in the study of Bagy, et al. [56], who reported that *Epicoccum nigrum* ASU11 served as a biocontrol agent against *Pectobacterium carotovora* subsp. *atrosepticum* PHY7, the bacterial strain responsible for the potato blackleg disease.

The use of nanoparticles in this study becomes important because of the wide range of fungi with diverse degrees of severity and specificity of action. This therefore calls for the use of a more ecofriendly control agent with a broader scope of action compared to the commonly use fungicide [57]. The similar pattern of performances expressed by the two nanoparticle types in the inhibition of fungal growths affirms their antifungal properties, and, as earlier reported, as safe and effective delivery systems of antifungal agents [58]. In this investigation, the results revealed *Phoma herbarium* as the most inhibited, followed by *A. alternata,* then *B. zeicola,* with *F. brachygibbosum* and *E. nigrum* showing the least inhibition, consistent with the properties of the fungi discussed earlier. *Phoma herbarium, A. alternata* and *B. zeicola* are endophytic pathogens that cause leaf spots and leaf blight diseases on maize plants [45,49,51,59]. On the other hand, *F. brachygibbosum* and *E. nigrum,* which were the least inhibited, could possibly exhibit biocontrol potentials [49,53]. The efficacy of the nanoparticles was observed to increase with increasing concentration levels, which is consistent with the earlier report of Kim, et al. [60] that AgNPs possess antifungal properties which were effective against the 18 tested plant pathogens at various levels. However, Bi_2S_3 nanoparticles were more effective at the lower concentration (5 mg/mL), as similarly recorded with sulphur nanoparticles where the fungal growths were hampered at 1500–3000 µg/mL concentration levels. Hence, the efficacy of sulphur nanoparticles was reported to be directly proportional to a reduction in the particle size [61]. The effectiveness of gC_3N_4 nanoparticles at higher concentrations (10 mg/mL and 15 mg/mL) could further substantiate its earlier-reported antifungal potentials [39]. Furthermore, the two nanoparticle types used in this study have been reported for their safety to humans, because of having little or no toxicity to cells as evident in their use in tomography imaging [57,62].

7. Conclusions

Foliar fungal pathogens isolated from the diseased maize leaves in this study were characterized as *Bipolaris zeicola, Phoma herbarum, Epicoccum nigrum, Alternaria alternata* and *Fusarium brachygibbosum.* Except *Epicoccum nigrum,* the fungal species were pathogens causing diseases such as leaf blight, leaf spot, wilting and stalk rot. *Phoma herbarium* > *A. alternata* > *B. zeicola* > *F. brachygibbosum* > *E. nigrum* was the order of percentage fungal inhibition by the nanoparticles. Bi_2S_3 was more effective against the pathogens at lower concentrations and gC_3N_4 at higher concentration levels. The two nanoparticle types evaluated in vitro show potential in managing these foliar pathogens, and this needs to be further validated in field studies. Other non-toxic nanoparticles could also be investigated against different fungal infections of plants. In addition, the mechanism of the interactions between the nanoparticles and the plants' fungi should be studied by using different char-

acterization tools. The effects of changes in nanoparticle morphologies on their antifungal performance is worth studying.

Author Contributions: Conceptualization, O.O.B., A.O.A., T.O.A. Methodology, A.O.A., T.O.A., M.S., S.D.M., D.C.O. and O.O.B. Software, A.O.A. and T.O.A. Validation, O.O.B., S.D.M., D.C.O. Formal analysis, A.O.A., T.O.A. Investigation, A.O.A., T.O.A., M.S., S.D.M., D.C.O. and O.O.B. Resources, O.O.B. and D.C.O. Data curation, A.O.A., T.O.A. and O.O.B. Writing—original draft, A.O.A., T.O.A., M.S. Writing—review & editing, A.O.A., T.O.A., M.S., S.D.M., D.C.O. and O.O.B. Visualization, A.O.A., T.O.A., M.S. Supervision, A.O.A., T.O.A. and O.O.B. Project administration, O.O.B., D.C.O., S.D.M. Funding acquisition, O.O.B. All authors have read and agreed to the published version of the manuscript.

Funding: O.O.B. recognizes the National Research Fund (NRF South Africa) for grants (UID123634 and UID132595) that support work in her research group.

Institutional Review Board Statement: This study did not require ethical approval.

Informed Consent Statement: Not applicable.

Data Availability Statement: The consensus nucleotide sequence data from this investigation were deposited in GenBank with accession numbers OP536174–OP536199.

Acknowledgments: North-West University, South Africa, is acknowledged for the postdoctoral funding awarded to A.O.A.; Nelson Mandela University, South Africa, is acknowledged for the postdoctoral grant awarded to T.O.A.

Conflicts of Interest: The authors declare no conflict of interest.

Abbreviations

Bi_2S_3	Bismuth sulphide nanoparticles
DNA	Deoxyribonucleic acid
EDS	Energy-dispersive X-ray spectroscopy
gC_3N_4	Graphitic carbon nitride nanoparticles
ITS	Internal transcribed spacer
NaOCl	Sodium hypochlorite
NCBI	National Center for Biotechnology Information
NH_4OH	Ammonium hydroxide solution
PCR	Polymerase chain reaction
PDA	Potato dextrose agar
rRNA	Ribosomal RNA
TEM	Transmission electron microscopy
XRD	X-ray diffraction

References

1. Tiwari, Y.K.; Yadav, S.K. High temperature stress tolerance in maize (*Zea mays* L.): Physiological and molecular mechanisms. *J. Plant Biol.* **2019**, *62*, 93–102. [CrossRef]
2. Ngoune, T.L.; Mutengwa, C.S. Estimation of maize (*Zea mays* L.) yield per harvest area: Appropriate methods. *Agronomy* **2019**, *10*, 29. [CrossRef]
3. Javed, T.; Shabbir, R.; Tahir, A.; Ahmar, S.; Mora-Poblete, F.; Razzaq, M.; Javed, Z.Q.; Zaghum, M.J.; Hussain, S.; Mukhtar, A. Etiology, Epidemiology, and Management of Maize Diseases. In *Cereal Diseases: Nanobiotechnological Approaches for Diagnosis and Management*; Springer: Berlin/Heidelberg, Germany, 2022; pp. 53–82.
4. Nji, Q.N.; Babalola, O.O.; Mwanza, M. Aflatoxins in maize: Can their occurrence be effectively managed in Africa in the face of climate change and food insecurity? *Toxins* **2022**, *14*, 574. [CrossRef] [PubMed]
5. Fones, H.N.; Bebber, D.P.; Chaloner, T.M.; Kay, W.T.; Steinberg, G.; Gurr, S.J. Threats to global food security from emerging fungal and oomycete crop pathogens. *Nat. Food* **2020**, *1*, 332–342. [CrossRef]
6. van der Does, H.C.; Rep, M. Virulence genes and the evolution of host specificity in plant-pathogenic fungi. *Mol. Plant-Microbe Interact.* **2007**, *20*, 1175–1182. [CrossRef]
7. Akanmu, A.O.; Sobowale, A.A.; Abiala, M.A.; Olawuyi, O.J.; Odebode, A.C. Efficacy of biochar in the management of *Fusarium verticillioides* Sacc. causing ear rot in *Zea mays* L. *Biotechnol. Rep.* **2020**, *26*, e00474. [CrossRef]

8. Belisário, R.; Robertson, A.E.; Vaillancourt, L.J. Maize anthracnose stalk rot in the genomic era. *Plant Dis.* **2022**, *106*, 2281–2298. [CrossRef]
9. Mesterhazy, A.; Szieberth, D.; Toldine, E.T.; Nagy, Z.; Szabó, B.; Herczig, B.; Bors, I.; Tóth, B. Updating the Methodology of Identifying Maize Hybrids Resistant to Ear Rot Pathogens and Their Toxins—Artificial Inoculation Tests for Kernel Resistance to Fusarium graminearum, F. verticillioides, and Aspergillus flavus. *J. Fungi* **2022**, *8*, 293. [CrossRef]
10. Xavier, F.; Kaushik, M. Biological management of charcoal rot of maize caused by Macrophomina phaseolina by using Trichoderma: A. *Pharma. Innov. J* **2021**, *10*, 417–441.
11. ur Rehman, F.; Adnan, M.; Kalsoom, M.; Naz, N.; Husnain, M.G.; Ilahi, H.; Ilyas, M.A.; Yousaf, G.; Tahir, R.; Ahmad, U. Seed-borne fungal diseases of Maize (*Zea mays* L.): A review. *Agrinula J. Agroteknologi Dan Perkeb.* **2021**, *4*, 43–60. [CrossRef]
12. Ferris, A.C.; Walbot, V. Understanding ustilago maydis infection of multiple maize organs. *J. Fungi* **2020**, *7*, 8. [CrossRef]
13. Akanmu, A.O.; Babalola, O.O.; Venturi, V.; Ayilara, M.S.; Adeleke, B.S.; Amoo, A.E.; Sobowale, A.A.; Fadiji, A.E.; Glick, B.R. Plant Disease Management: Leveraging on the Plant-Microbe-Soil Interface in the Biorational Use of Organic Amendments. *Front. Plant Sci.* **2021**, *12*, 1590. [CrossRef]
14. Sibiya, M.; Sumbwanyambe, M. A computational procedure for the recognition and classification of maize leaf diseases out of healthy leaves using convolutional neural networks. *AgriEngineering* **2019**, *1*, 119–131. [CrossRef]
15. Kotze, R.; Van der Merwe, C.; Crampton, B.; Kritzinger, Q. A histological assessment of the infection strategy of Exserohilum turcicum in maize. *Plant Pathol.* **2019**, *68*, 504–512. [CrossRef]
16. Craven, M.; Morey, L.; Abrahams, A.; Njom, H.A.; van Rensburg, B.J. Effect of northern corn leaf blight severity on Fusarium ear rot incidence of maize. *South Afr. J. Sci.* **2020**, *116*, 11–12. [CrossRef]
17. Latterell, F.M.; Rossi, A.E. Gray leaf spot of corn: A disease on the move. *Plant Dis.* **1983**, *67*, 842–847. [CrossRef]
18. Degani, O.; Gordani, A.; Becher, P.; Chen, A.; Rabinovitz, O. Crop rotation and minimal tillage selectively affect maize growth promotion under late wilt disease stress. *J. Fungi* **2022**, *8*, 586. [CrossRef]
19. Fadiji, A.E.; Ayangbenro, A.S.; Babalola, O.O. Organic farming enhances the diversity and community structure of endophytic archaea and fungi in maize plant: A shotgun approach. *J. Soil Sci. Plant Nutr.* **2020**, *20*, 2587–2599. [CrossRef]
20. Fasusi, O.A.; Cruz, C.; Babalola, O.O. Agricultural sustainability: Microbial biofertilizers in rhizosphere management. *Agriculture* **2021**, *11*, 163. [CrossRef]
21. Gossen, B.D.; McDonald, M.R. New technologies could enhance natural biological control and disease management and reduce reliance on synthetic pesticides. *Can. J. Plant Pathol.* **2020**, *42*, 30–40. [CrossRef]
22. Wise, K.; Mueller, D. Are Fungicides No Longer Just for Fungi? An Analysis of Foliar Fungicide Use in Corn. Available online: https://www.apsnet.org/edcenter/apsnetfeatures/Pages/fungicide.aspx (accessed on 7 March 2023).
23. Olowe, O.M.; Nicola, L.; Asemoloye, M.D.; Akanmu, A.O.; Babalola, O.O. Trichoderma: Potential bio-resource for the management of tomato root rot diseases in Africa. *Microbiol. Res.* **2022**, *257*, 126978. [CrossRef] [PubMed]
24. Rani, L.; Thapa, K.; Kanojia, N.; Sharma, N.; Singh, S.; Grewal, A.S.; Srivastav, A.L.; Kaushal, J. An extensive review on the consequences of chemical pesticides on human health and environment. *J. Clean. Prod.* **2021**, *283*, 124657. [CrossRef]
25. Hammami, I.; Alabdallah, N.M. Gold nanoparticles: Synthesis properties and applications. *J. King Saud Univ.-Sci.* **2021**, *33*, 101560. [CrossRef]
26. Ajilogba, C.F.; Babalola, O.O.; Nikoro, D.O. Nanotechnology as vehicle for biocontrol of plant diseases in crop production. In *Food Security and Safety*; Springer: Cham, Switzerland, 2021; pp. 709–724.
27. Younas, A.; Yousaf, Z.; Rashid, M.; Riaz, N.; Fiaz, S.; Aftab, A.; Haung, S. Nanotechnology and plant disease diagnosis and management. In *Nanoagronomy*; Springer: Cham, Switzerland, 2020; pp. 101–123.
28. Fadiji, A.E.; Mortimer, P.E.; Xu, J.; Ebenso, E.E.; Babalola, O.O. Biosynthesis of nanoparticles using endophytes: A novel approach for enhancing plant growth and sustainable agriculture. *Sustainability* **2022**, *14*, 10839. [CrossRef]
29. Imade, E.E.; Ajiboye, T.O.; Fadiji, A.E.; Onwudiwe, D.C.; Babalola, O.O. Green synthesis of zinc oxide nanoparticles using plantain peel extracts and the evaluation of their antibacterial activity. *Sci. Afr.* **2022**, *16*, e01152. [CrossRef]
30. Li, Y.; Zhang, P.; Li, M.; Shakoor, N.; Adeel, M.; Zhou, P.; Guo, M.; Jiang, Y.; Zhao, W.; Lou, B.; et al. Application and mechanisms of metal-based nanoparticles in the control of bacterial and fungal crop diseases. *Pest Manag. Sci.* **2023**, *79*, 21–36. [CrossRef]
31. Daccò, C.; Nicola, L.; Temporiti, M.E.E.; Mannucci, B.; Corana, F.; Carpani, G.; Tosi, S. Trichoderma: Evaluation of its degrading abilities for the bioremediation of hydrocarbon complex mixtures. *Appl. Sci.* **2020**, *10*, 3152. [CrossRef]
32. Mansoor Ali, S.; Aldawood, S.; AlGarawi, M.S.; AlGhamdi, S.S.; Kassim, H.; Aziz, A. Influence of gamma irradiation on structural, optical, and electrical characterization of Bi2S3 thin films. *J. Mater. Sci. Mater. Electron.* **2022**, *33*, 18982–18990. [CrossRef]
33. Cheng, D.; Wu, H.; Feng, C.; Ding, Y.; Mei, H. Bifunctional photoelectrochemical sensor based on Bi/Bi2S3/BiVO4 for detecting hexavalent chromium and hydrogen peroxide. *Sens. Actuators B Chem.* **2022**, *353*, 131108. [CrossRef]
34. Zhang, H.; Wang, L. Synthesis and characterization of Bi2S3 nanorods by solvothermal method in polyol media. *Mater. Lett.* **2007**, *61*, 1667–1670. [CrossRef]
35. Imam, S.S.; Adnan, R.; Mohd Kaus, N.H. Room-temperature synthesis of flower-like BiOBr/Bi2S3 composites for the catalytic degradation of fluoroquinolones using indoor fluorescent light illumination. *Colloids Surf. A Physicochem. Eng. Asp.* **2020**, *585*, 124069. [CrossRef]
36. Ajiboye, T.O.; Kuvarega, A.T.; Onwudiwe, D.C. Graphitic carbon nitride-based catalysts and their applications: A review. *Nano-Struct. Nano-Objects* **2020**, *24*, 100577. [CrossRef]

37. Gashi, A.; Parmentier, J.; Fioux, P.; Marsalek, R. Tuning the C/N Ratio of C-Rich Graphitic Carbon Nitride (g-C3N4) Materials by the Melamine/Carboxylic Acid Adduct Route. *Chem.—A Eur. J.* **2022**, *28*, e202103605. [CrossRef]
38. Ajiboye, T.O.; Oyewo, O.A.; Marzouki, R.; Onwudiwe, D.C. Photocatalytic Reduction of Hexavalent Chromium Using Cu3.21Bi4.79S9/g-C3N4 Nanocomposite. *Catalysts* **2022**, *12*, 1075. [CrossRef]
39. Ajiboye, T.O.; Imade, E.E.; Oyewo, O.A.; Onwudiwe, D.C. Silver functionalized gC3N4: Photocatalytic potency for chromium(VI) reduction, and evaluation of the antioxidant and antimicrobial properties. *J. Photochem. Photobiol. A Chem.* **2022**, *432*, 114107. [CrossRef]
40. Akanmu, A.O.; Odebode, A.C.; Abiala, M.A.; Aiyelaagbe, O.O.; Olaoluwa, O.O. Inhibition of Fusarium pathogens in millet by extracts of Jatropha curcas and Mangifera indica. *Int. J. Plant Biol. Res.* **2014**, *2*, 1007.
41. Olowe, O.M.; Nicola, L.; Aemoloye, M.D.; Akanmu, A.O.; Sobowale, A.A.; Babalola, O.O. Characterization and antagonistic potentials of selected rhizosphere Trichoderma species against some Fusarium species. *Front. Microbiol.* **2022**, *13*, 3757. [CrossRef]
42. Dodd, J. Recent developments in the maize pathogen Bipolaris zeicola Shoemaker. *Maydica* **1993**, *38*, 201–204.
43. Tsukiboshi, T.; Kimigafukuro, T.; Sato, T. Identification of races of Bipolaris zeicola, the causal fungus of Helminthosporium leaf spot on corn in Japan. *Jpn. J. Phytopathol.* **1987**, *53*, 647–649. [CrossRef]
44. Liu, S.; Guo, N.; Ma, H.; Sun, H.; Zheng, X.; Shi, J. First Report of Root Rot Caused by Bipolaris zeicola on Maize in Hebei Province. *Plant Dis.* **2021**, *105*, 2247. [CrossRef]
45. Sun, X.; Qi, X.; Wang, W.; Liu, X.; Zhao, H.; Wu, C.; Chang, X.; Zhang, M.; Chen, H.; Gong, G. Etiology and symptoms of maize leaf spot caused by Bipolaris spp. in Sichuan, China. *Pathogens* **2020**, *9*, 229. [CrossRef] [PubMed]
46. Kleczewski, N.M.; Flory, S.L. Leaf blight disease on the invasive grass Microstegium vimineum caused by a *Bipolaris* sp. *Plant Dis.* **2010**, *94*, 807–811. [CrossRef] [PubMed]
47. Deb, D.; Khan, A.; Dey, N. Phoma diseases: Epidemiology and control. *Plant Pathol.* **2020**, *69*, 1203–1217. [CrossRef]
48. Zhang, Y.; Crous, P.W.; Schoch, C.L.; Hyde, K.D. Pleosporales. *Fungal Divers.* **2012**, *53*, 1–221. [CrossRef]
49. Garibaldi, A.; Gilardi, G.; Matic, S.; Gullino, M. First Report of Phoma herbarum Causing Leaf Spot of Purple Coneflower (*Echinacea purpurea*) in Northern Italy. *Plant Dis.* **2019**, *103*, 1786. [CrossRef]
50. Higgins, K.L.; Arnold, A.E.; Coley, P.D.; Kursar, T.A. Communities of fungal endophytes in tropical forest grasses: Highly diverse host-and habitat generalists characterized by strong spatial structure. *Fungal Ecol.* **2014**, *8*, 1–11. [CrossRef]
51. Xu, X.; Zhang, L.; Yang, X.; Cao, H.; Li, J.; Cao, P.; Guo, L.; Wang, X.; Zhao, J.; Xiang, W. *Alternaria* spp. associated with leaf blight of maize in Heilongjiang Province, China. *Plant Dis.* **2022**, *106*, 572–584. [CrossRef]
52. Kgatle, M.G.; Truter, M.; Ramusi, T.; Flett, B.; Aveling, T. Alternaria alternata, the causal agent of leaf blight of sunflower in South Africa. *Eur. J. Plant Pathol.* **2018**, *151*, 677–688. [CrossRef]
53. Rna, A.; Babikar, A.; Dagash, Y.; Elhussein, A.; Elhalim, T.; Babikar, A. Fusarium Brachygibbosum a Plausible Candidate for Deployment as a Bioagent for Striga Hermonthica Management in Sorghum. In Proceedings of the Third Conference of Pests Management in Sudan February, Wad Medani, Sudan, 3–4 February 2014; pp. 3–4.
54. Shan, L.; Cui, W.; Zhang, D.; Zhang, J.; Ma, N.; Bao, Y.; Dai, X.; Guo, W. First report of Fusarium brachygibbosum causing maize stalk rot in China. *Plant Dis.* **2017**, *101*, 837. [CrossRef]
55. Taguiam, J.D.; Evallo, E.; Balendres, M.A. Epicoccum species: Ubiquitous plant pathogens and effective biological control agents. *Eur. J. Plant Pathol.* **2021**, *159*, 713–725. [CrossRef]
56. Bagy, H.M.K.; Hassan, E.A.; Nafady, N.A.; Dawood, M.F. Efficacy of arbuscular mycorrhizal fungi and endophytic strain Epicoccum nigrum ASU11 as biocontrol agents against blackleg disease of potato caused by bacterial strain Pectobacterium carotovora subsp. atrosepticum PHY7. *Biol. Control* **2019**, *134*, 103–113. [CrossRef]
57. Abdel-Moniem, S.M.; El-Liethy, M.A.; Ibrahim, H.S.; Ali, M.E. Innovative green/non-toxic Bi2S3@ g-C3N4 nanosheets for dark antimicrobial activity and photocatalytic depollution: Turnover assessment. *Ecotoxicol. Environ. Saf.* **2021**, *226*, 112808. [CrossRef]
58. Soliman, G.M. Nanoparticles as safe and effective delivery systems of antifungal agents: Achievements and challenges. *Int. J. Pharm.* **2017**, *523*, 15–32. [CrossRef]
59. Hamayun, M.; Khan, S.A.; Khan, A.L.; Rehman, G.; Sohn, E.-Y.; Shah, A.A.; Kim, S.-K.; Joo, G.-J.; Lee, I.-J. Phoma herbarum as a new gibberellin-producing and plant growth-promoting fungus. *J. Microbiol. Biotechnol.* **2009**, *19*, 1244–1249.
60. Kim, S.W.; Jung, J.H.; Lamsal, K.; Kim, Y.S.; Min, J.S.; Lee, Y.S. Antifungal effects of silver nanoparticles (AgNPs) against various plant pathogenic fungi. *Mycobiology* **2012**, *40*, 53–58. [CrossRef]
61. Rai, M.; Ingle, A.P.; Paralikar, P. Sulfur and sulfur nanoparticles as potential antimicrobials: From traditional medicine to nanomedicine. *Expert Rev. Anti-Infect. Ther.* **2016**, *14*, 969–978. [CrossRef]
62. Rajiv, P.; Mengelizadeh, N.; McKay, G.; Balarak, D. Photocatalytic degradation of ciprofloxacin with Fe_2O_3 nanoparticles loaded on graphitic carbon nitride: Mineralisation, degradation mechanism and toxicity assessment. *Int. J. Environ. Anal. Chem.* **2021**, 1–15. [CrossRef]